IEEE Access
Multidisciplinary | Rapid Review | Open Access Journal

Received April 18, 2022, accepted April 25, 2022, date of publication April 29, 2022, date of current version May 9, 2022.

*Digital Object Identifier 10.1109/ACCESS.2022.3171247*

# Macroscopic Big Data Analysis and Prediction of Driving Behavior With an Adaptive Fuzzy Recurrent Neural Network on the Internet of Vehicles

**DAVID CHUNHU LI[1], (Member, IEEE), MICHAEL YU-CHING LIN[1], AND LI-DER CHOU[2], (Member, IEEE)**

[1]Information Technology and Management Program, Ming Chuan University, Taoyuan 33332, Taiwan
[2]Department of Computer Science and Information Engineering, National Central University, Taoyuan 32031, Taiwan

Corresponding author: David Chunhu Li (davidli@mail.mcu.edu.tw)

This work was supported in part by the Ming Chuan University Research Fund of 110 Academic Year, and in part by the Ministry of Science and Technology of Taiwan under Grant 108-2221-E-008-033-MY3 and Grant 110-2218-E-415-001-MBK.

**ABSTRACT** Dangerous driving behaviors are diverse and complex. Determining how to analyze the driving behavior of public drivers objectively and accurately has always been a research challenge. This research proposes a macroscopic and dynamic method for evaluating drivers' dangerous driving degree based on a fuzzy inference system. It also designs fuzzy-macro long short-term memory (LSTM), a variant of LSTM recurrent neural networks, which can predict drivers' dangerous driving behaviors and risk degree. We elucidate how a macroscopic fuzzy inference dangerous driving behavior system is designed based on various driving behavior factors and the neuron architecture of the fuzzy-macro LSTM network. We collect real driving behavior data of drivers on the road and conduct a series of experimental analyses. Compared with five other commonly used time-series forecasting neural network models, our fuzzy-macro LSTM model performs best in terms of prediction error. Experimental results verify the effectiveness of the proposed method for macroanalysis and prediction of dangerous driving behavior.

**INDEX TERMS** Data analysis, time series, fuzzy rules, driving behavior, prediction, fuzzy neural network.

## I. INTRODUCTION

The Internet of Vehicles (IoV) is an innovative networking service of the Internet of Things for the motor vehicle industry. People install devices on vehicles to collect and send data to a cloud computing platform for further data analysis and processing. Various car networking services, such as usage-based insurance (UBI), intelligent transportation system, and smart navigation, have been created to provide people with a highly comfortable driving environment and a rich and diverse driving experience [1]. The analysis of driving behavior has always been an important research topic in the field of IoV [2], [3]. Accident prevention, driving style assessment, UBI, fleet management, and driver intent prediction are typical IoV applications based on big data analysis of driving behavior. Such applications collect a massive amount of data from drivers' smartphones, car driving recorders, in-vehicle infotainment devices, and on-board diagnostics (OBD)-II adapters in vehicles through wireless networking. IoV application users then analyze the collected data on a cloud computing platform by using big data analysis, machine learning, and deep learning models [4], [5].

Machine learning is one of the important research methods for driving behavior analysis and prediction. People train various machine learning or deep learning models to learn and label dangerous driving features to classify or predict driving behaviors [6]–[8]. Machine learning-based methods must collect and analyze various data to train the models. However, many of the motor vehicles currently running on the road are ordinary vehicles. These aftermarket nonluxury vehicles do not have data collection devices, such as advanced driver assistance systems (ADAS), driving recorders, or cameras preinstalled. The installation of various driving recorders, ADAS, and cameras on vehicles is not only expensive but

The associate editor coordinating the review of this manuscript and approving it for publication was Muhammad Zakarya.

also complicated [9]. Installing excessive external electrical equipment on a vehicle will also cause a heavy electrical load and fire hazards [10]. With these aforementioned factors, various driving behavior detection technologies designed based on sensing devices, such as ADAS, cameras, and video recorders, cannot be used widely.

Studies on how to analyze and predict driving behaviors by using various physiological sensing devices attached to a driver's body have also been conducted. These studies used intrusive data collection methods that collect and analyze the driver's physical physiological data to determine whether the driver has distracted driving and fatigued driving behavior [11]–[13]. However, drivers may be reluctant to install these devices in practice because of concerns that the physiological sensing devices will affect their driving. At present, most ordinary vehicles in the aftermarket still lack easy-to-use and cost-effective technologies and methods to detect and prevent dangerous driving behaviors. Thus, more advanced technologies should be explored to protect drivers' safety.

To tackle the aforementioned challenges, this study aims to integrate big data analysis, fuzzy theory, and deep learning to address the critical problems in driving behavior analysis and prediction. The major contributions of this work can be summarized as follows:

1) We review the main methods for identification and analysis of driving behavior on IoV, discuss the characteristics of these methods, and propose important issues to be solved.
2) We propose a novel method for macro data analysis to assess drivers' degree of dangerous driving. We also design a fuzzy inference system, which can flexibly incorporate various driving behaviors of drivers into factors, for evaluating dangerous driving behavior and the degree of macro driving risk.
3) We propose a fuzzy-macro long short-term memory (LSTM) model, which is a variant of the recurrent neural network (RNN) model and can predict the degree of macro dangerous driving behavior. We describe the architectural design of the neural unit of the neural network model.
4) We perform a series of multifaceted experimental analyses. The experimental results prove the effectiveness of the macroscopic dangerous driving behavior analysis and prediction model proposed in this research.

The remainder of this paper is organized as follows. Section II presents our research methods, describes the problem to be solved, and presents a novel fuzzy interference system and a fuzzy-macro LSTM model. Section III evaluates our models and discusses the experimental methods and results. Section IV discusses the research background and related work, and further reviews various major approaches that analyze driving behaviors. Section V concludes the study and presents suggestions for future work.

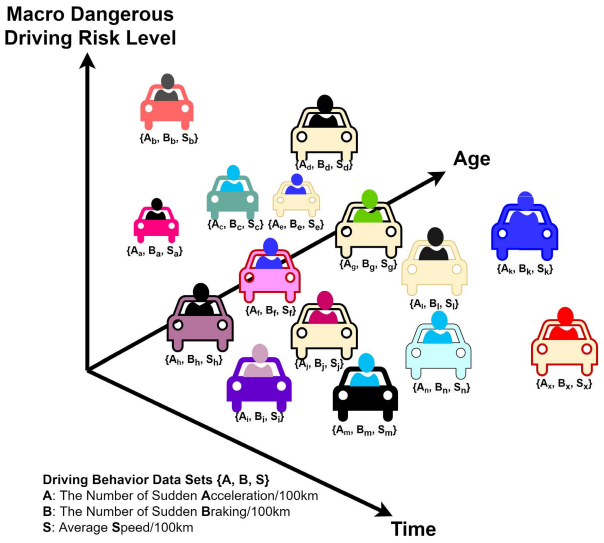


**FIGURE 1.** Illustration of problem definition.

## II. RESEARCH METHOD

In this section, we first describe the definition of the problem to be solved. Then, we propose a fuzzy logic system that assesses the risk of driving behavior from a macro level and a deep learning model that can predict the level of macro risk.

### A. PROBLEM STATEMENT

Drivers' driving habits and behaviors are diverse and complex. Drivers' degree of dangerous driving is difficult to assess based on certain driving behaviors. As shown in Figure 1, suppose a certain auto insurance company has millions of customers. Determining how to analyze the various driving behaviors of each driver from a macro perspective comprehensively and assess the risk of traffic accidents for all drivers accurately and objectively are problems that have an important commercial value and are worthy of in-depth study.

The problem of macroscopic analysis of driving behavior on IoV could be represented as (1). $\boldsymbol{y}_i$ is the driver's macro risky driving degree, and $f^*$ is a target function for calculating this macro risky driving degree. The input parameters of $f^*$ function are a set of driving behaviors, including the driver's number of sudden accelerations per 100 km, denoted as $\mathcal{X}_\mathcal{A}$; the number of sudden braking per 100 km, denoted as $\mathcal{X}_\mathcal{B}$; and the average speed per 100 km, denoted as $\mathcal{X}_\mathcal{S}$. $f^*$ is calculated by the fuzzy inference system of macro driving behavior designed in this work. In practical applications, users can flexibly add or replace various other driving behavior features in the set in accordance with their needs. This study currently uses only three important driving behaviors.

$$f^* : (\mathcal{X}_\mathcal{A}, \mathcal{X}_\mathcal{B}, \mathcal{X}_\mathcal{S}) \rightarrow \mathcal{Y},$$
$$\boldsymbol{y}_i = f^*\left(\boldsymbol{x}_{A_i}, \boldsymbol{x}_{B_i}, \boldsymbol{x}_{S_i}\right), \quad i = 1, \ldots, n. \tag{1}$$

The definition of predicting the degree of macroscopic risk is described in (2). $y_{pred}(t)$ is the predicted macroscopic comprehensive dangerous driving degree of the driver at a certain

time t, and $y_{pred}(t)$ is a multivariate time-series forecasting function to predict the macro risk level of vehicle drivers. The input parameter of $y_{pred}(t)$ is a 3D matrix of driving behavior data. The matrix consists of the number of sudden accelerations per 100 km, denoted as **A**; the number of sudden braking per 100 km, denoted as **B**; and the average speed per 100 km, denoted as **S**. $\alpha_i$, $\beta_i$, $\gamma_i$, and $\mu_i$ are the coefficients of the lag operation of the time-series model, and $\varepsilon$ is the residual of the lag operation. $y_{pred}(t)$ will be derived from the fuzzy-macro LSTM model that will be described in the following section.

$$\begin{aligned} & y_{pred}(t) \\ & = \text{argmax}\, P\left((\mathbf{A},\mathbf{B},\mathbf{S})_t \mid (\mathbf{A},\mathbf{B},\mathbf{S})_{t-T},\cdots,(\mathbf{A},\mathbf{B},\mathbf{S})_{t-1}\right) \\ & = \sum_{i=1}^{p} \Phi_i y_{pred}(t-i) + \sum_{i=0}^{k} \alpha_i x_{\mathbf{A}}(t-i) + \sum_{i=0}^{k} \beta_i x_{\mathbf{B}}(t-i) \\ & \quad + \sum_{i=0}^{k} \gamma_i x_{\mathbf{S}}(t-i) + \sum_{i=0}^{q} \mu_i \varepsilon(t-i) \end{aligned} \tag{2}$$

### B. FUZZY SET MODEL DESCRIPTION

We assume that the driving behavior data set $\mathbb{R}$ is a set of rational numbers. We define the macroscopic dangerous driving behavior fuzzy set $\tilde{A}$ in $\mathbb{R}$ as a set of ordered pairs, and $\tilde{A}$ is expressed as (3). Given that the driving behavior data are discrete and limited, the fuzzy set of macro dangerous driving behavior can be expressed as (4). $\eta_{\tilde{A}}(y)$ is the membership degree of y in the fuzzy set. $y_1$ is the performance degree of sudden acceleration per 100 km, $y_2$ is the performance degree of sudden braking per 100 km, and $y_3$ is the performance degree of average speed per 100 km.

$$\tilde{A} = \left\{(y, \eta_{\tilde{A}}(y)) | y \in \mathbb{R}\right\} \tag{3}$$

$$\begin{aligned} \tilde{A} &= \left\{\frac{\eta_{\tilde{A}}(y_1)}{y_1} + \frac{\eta_{\tilde{A}}(y_2)}{y_2} + \frac{\eta_{\tilde{A}}(y_3)}{y_3} + \cdots\right\} \\ &= \left\{\sum_{i=1}^{n} \frac{\eta_{\tilde{A}}(y_i)}{y_i}\right\} \end{aligned} \tag{4}$$

The calculation of $y_i$ is presented in (5), where $\rho$ is the percentage and $\lambda$ is the exponential distribution of $y_i$.

$$y_i(\rho, \lambda) = \frac{-ln(1-\rho)}{\lambda} \tag{5}$$

### C. FUZZY INTERFERENCE LOGIC RULES

The fuzzy rule library for macro driving behavior evaluation is composed of the following fuzzy IF-THEN rule set, as shown in (6). $A_n^i$ and $\theta^i$ are input and output fuzzy sets, respectively. $x \in \{x_1, x_2, \ldots, x_n\}$ and $y$ are the input and output of the fuzzy derivation system, respectively [14].

$$i^{th}\ rule: IF\ x_1\ is\ A_1^i, \ldots, and\ x_n\ is\ A_n^i, \quad THEN\ y = \theta^i \tag{6}$$

The fuzzy evaluation system of macro driving behavior in this study contains 3 input parameters, 1 output result, and 27 fuzzy rules. Table 1 shows the designed fuzzy rule library for macro driving behavior evaluation. It comprises three input parameters and one output value. The three input parameters are the number of sudden accelerations per 100 km (low, medium, high), the number of sudden braking per 100 km (low, medium, high), and the average speed per 100 km (low, medium, high). The output is the macroscopic dangerous driving degree (low, medium, high).

Let the fuzzy set of the degree of sudden acceleration per 100 km be $\tilde{E}$, the fuzzy set of the degree of sudden braking per 100 km be $\tilde{Z}$, and the fuzzy set of the average speed per 100 km be $\tilde{H}$. Then the macroscopic dangerous driving degree is given by (7).

$$\begin{aligned} \theta &= \mu_{\tilde{E}\cap\tilde{Z}\cap\tilde{H}}(x) = \wedge[\,\mu_{\tilde{E}}, \mu_{\tilde{Z}}, \mu_{\tilde{H}}] \\ &= min[\,\mu_{\tilde{E}}, \mu_{\tilde{Z}}, \mu_{\tilde{H}}] \end{aligned} \tag{7}$$

The calculation of fuzzy rule inference to evaluate the macro dangerous driving degree is shown in (8).

$$\begin{aligned} & R_1: IF\ x_1\ is\ \tilde{E}_{11}\ and\ x_2\ is\ \tilde{Z}_{12}\ and\ x_3\ is\ \tilde{H}_{13}, \\ & \qquad THEN\ \theta_1 = a_1 \times x_1 + b_1 \times x_2 + c_1 \times x_3 + d_1 \\ & R_2: IF\ x_1\ is\ \tilde{E}_{21}\ and\ x_2\ is\ \tilde{Z}_{22}\ and\ x_3\ is\ \tilde{H}_{23}, \\ & \qquad THEN\ \theta_2 = a_2 \times x_1 + b_2 \times x_2 + c_2 \times x_3 + d_2 \\ & R_i: IF\ x_1\ is\ \tilde{E}_{i1}\ and\ x_2\ is\ \tilde{Z}_{i2}\ and\ x_3\ is\ \tilde{H}_{i3}, \\ & \qquad THEN\ \theta_i = a_i \times x_1 + b_i \times x_2 + c_i \times x_3 + d_i \end{aligned} \tag{8}$$

The fuzzy evaluation system will synthesize all the rules and defuzzify them by using the weighted average method to calculate a fuzzy system output value $\theta^0$, as shown in (9), where $w_i$ is the suitability of each rule.

$$\begin{aligned} \theta^0 &= \frac{\left(\sum_{i=1}^{n} w_i \times \theta_i\right)}{\sum_{i=1}^{n} w_i},\ where \\ w_i &= \mu_{\tilde{E}_{i1}}(x_1^0) \wedge \mu_{\tilde{Z}_{i1}}(x_1^0) \wedge \mu_{\tilde{H}_{i1}}(x_1^0) \end{aligned} \tag{9}$$

Figure 2 shows the distribution diagram of the membership function of the designed fuzzy evaluation system for macro analysis of dangerous driving behavior. In a fuzzy membership function graph, the vertical axis is a number between 0 and 1, and is called the membership value. The horizontal axis is a set of real numbers that map to membership values. In Figure 2, the horizontal axis is a set of normalized real driving behavior values (such as the number of sudden braking per 100 km, the number of sudden acceleration per 100 km, and the average speed per 100 km), and the vertical axes are the membership values of performance level that are mapped to each dangerous driving behavior when the set of driving behaviors is applied with fuzzy set rules.

Figure 3 presents a 3D surface plot of the macroscopic fuzzy evaluation system. The plane coordinate axes in the 3D graph in Figure 3 represent the normalized driver's number of sudden accelerations and sudden brakings per 100 km, respectively. The vertical axis in the 3D graph represents the derived membership value of the degree of macroscopic dangerous driving behavior, which refers to the change of the area in the 3D graph. In Figure 3, we use the grid values of the degree of sudden acceleration and sudden braking of

**TABLE 1. Macro driving behavior fuzzy interference system rules.**

| Rule Number | Number of Sudden Acceleration | Number of Sudden Braking | Average Speed | Macro Dangerous Driving Degree |
|---|---|---|---|---|
| 1 | High | High | High | High |
| 2 | High | High | Medium | High |
| 3 | High | High | Low | High |
| 4 | High | Medium | High | High |
| 5 | High | Medium | Medium | Medium |
| 6 | High | Medium | Low | Medium |
| 7 | High | Low | High | High |
| 8 | High | Low | Medium | Medium |
| 9 | High | Low | Low | Low |
| 10 | Medium | High | High | High |
| 11 | Medium | High | Medium | Medium |
| 12 | Medium | High | Low | Medium |
| 13 | Medium | Medium | High | Medium |
| 14 | Medium | Medium | Medium | Medium |
| 15 | Medium | Medium | Low | Medium |
| 16 | Medium | Low | High | Medium |
| 17 | Medium | Low | Medium | Medium |
| 18 | Medium | Low | Low | Low |
| 19 | Low | High | High | High |
| 20 | Low | High | Medium | Medium |
| 21 | Low | High | Low | Low |
| 22 | Low | Medium | High | Medium |
| 23 | Low | Medium | Medium | Medium |
| 24 | Low | Medium | Low | Low |
| 25 | Low | Low | High | Low |
| 26 | Low | Low | Medium | Low |
| 27 | Low | Low | Low | Low |

1000 drivers per 100 km as the system input, and the estimated macroscopic dangerous driving degree of the drivers is the surface output value. We illustrate the use case of the designed fuzzy evaluation system in Figure 4. The horizontal axis in Figure 4 is the fuzzy inference system's support for the derived macroscopic dangerous driving behavior degree, which refers to the red-filled area characterized by full membership in the fuzzy set. The vertical axis is the membership value of the macroscopic dangerous driving degree, which is between 0 and 1. We analyze the driving behavior of a 38-year-old man. His sudden acceleration degree per 100 km is 87%, the sudden braking degree per 100 km is 93.6%, and the average speed degree per 100 km is 95.7%. The system estimates that his macro dangerous driving behavior is 92%, which implies high-risk dangerous driving. Accordingly, our fuzzy evaluation system can achieve a macroscopic analysis of the degree of dangerous driving behavior of all drivers in different age groups, genders, and periods.

### D. FUZZY-MACRO LSTM

We assume that the driving behavior and vehicle condition data are time-series data. We can use RNNs to track time-series data up to the time we observed the data. An RNN has a "state" for storing information related to the information observed and processed so far, and it can process sequential data through multiple iterations [15]. An LSTM network enhances the short-term memory in RNNs [16]. It is currently widely used in natural language processing, image recognition, and other applications due to its strong reconnaissance capability [17]–[20]. We propose fuzzy-macro LSTM, a deep learning model based on LSTM RNNs, in this work. We represent daily driving behavior with a time-series data structure of a 3D matrix, as shown in Figure 5, and design a variant of LSTM models to learn driving behavior patterns and predict the macro risk level of dangerous driving. In Figure 5, NOST/100 km represents the number of sharp turns the driver makes per 100 km. FC/100 km refers to the fuel consumption of the driver per 100 km. AS/100 km refers to the average speed of the driver per 100 km. NOSB/100 km represents the number of sudden braking per 100 km by the driver. NOSA/100 km refers to the number of sudden acceleration per 100km by the driver.

The LSTM network can effectively solve the problem of the vanishing gradient of the traditional RNN network, and it can learn to remember a single event that occurs in a long time series and adjust the oscillation of the signal in non-stationary data. However, training LSTM network models requires complex data preparation. For example, to ensure that the LSTM network focuses on underlying signals in time series, machine learning practitioners need to remove periodic and trending signals in the data for training LSTM network models. This step can lead to decreased performance of LSTMs in predicting trend problems. Furthermore, LSTM networks require a large amount of training resources and time to learn nonlinear predictive relationships in big data sensed by IoV. This study aims to address the question of how various risky driving behaviors and trends in macroscopic risk levels can be predicted in a cost-effective manner. To maintain high predictive power with less computational resources and training time, the internal architecture of the LSTM unit is fine-tuned to make the LSTM network more suitable for addressing the problem to be solved in this work. Figure 6 shows the neural unit structure of the fuzzy-macro LSTM model. The model unit contains a forget gate layer, an input gate layer, and an output gate layer. $c_{t-1}$ is the output of the previous model neural unit, $c_t$ is the output of the current model neural unit, and $h_t$ is the final state. Given the input $\mathbb{N}_{\text{seq}}$, the previous state $h_{t-1}$, and the previous unit output $c_{t-1}$, the fuzzy-macro LSTM unit records historical driving behavior characteristic information, and the unit update interval is t. When a new driving behavior feature vector is input, the forget gate layer decides which information will be deleted. Among them, $\mathbb{N}_{\text{seq}}$ is the vector of various dangerous driving behaviors, and $R_{level}$ is the level of dangerous driving evaluated using the macro-fuzzy logic analysis subsystem. Given that the degree of macro dangerous driving reflects the driver's long-term dangerous driving behavior, the degree of dangerous driving is separately introduced into the input, output, and forget gates in the fuzzy-macro LSTM network unit to deepen the memory of the driver's historical degree of dangerous driving behavior and avoid being forgotten by the forget gate. When the new time-series driving behaviors are input into the model, outdated information will be eliminated by the forget gate. The output $f_t$ of the forget gate is expressed in (10), where $\varphi$ is the sigmoid function, $W_f$ is the weight matrix of the forget gate layer, and $b_f$ is the deviation value

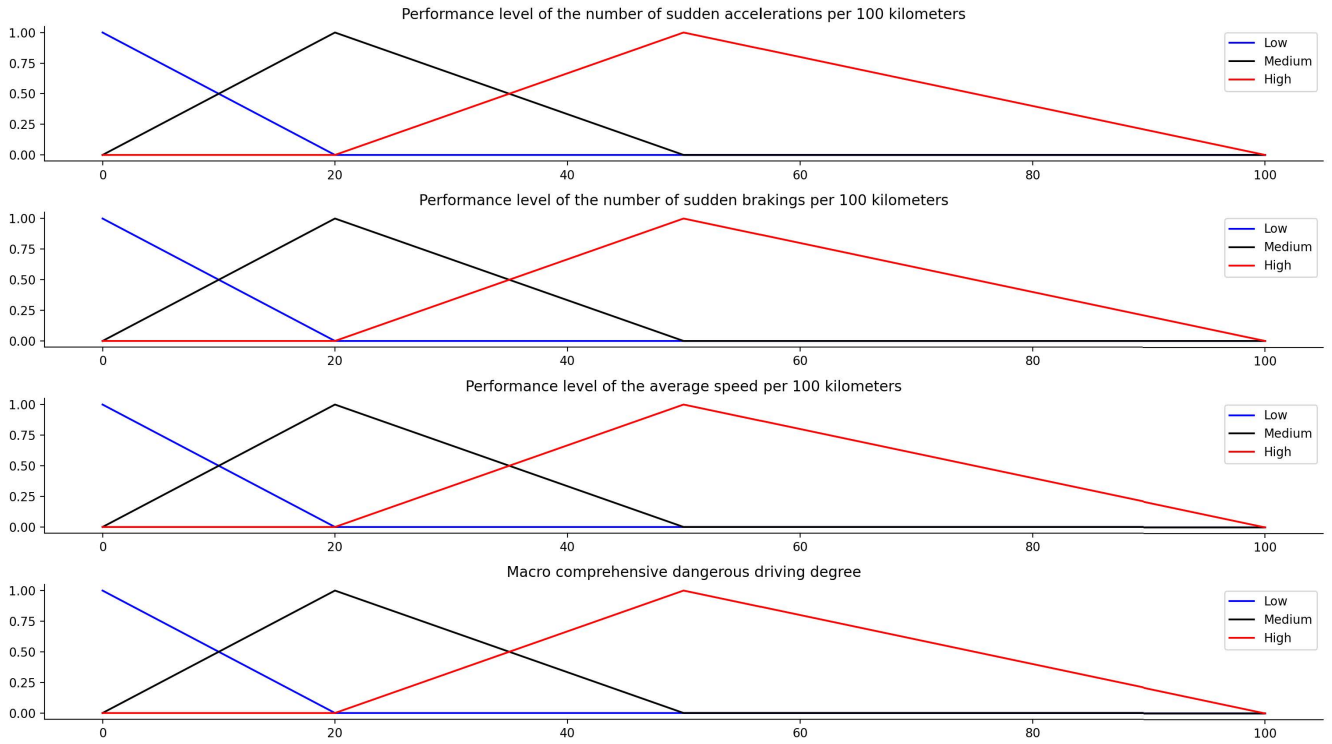


**FIGURE 2.** Membership function distributions of the macro driving behavior fuzzy inference system.

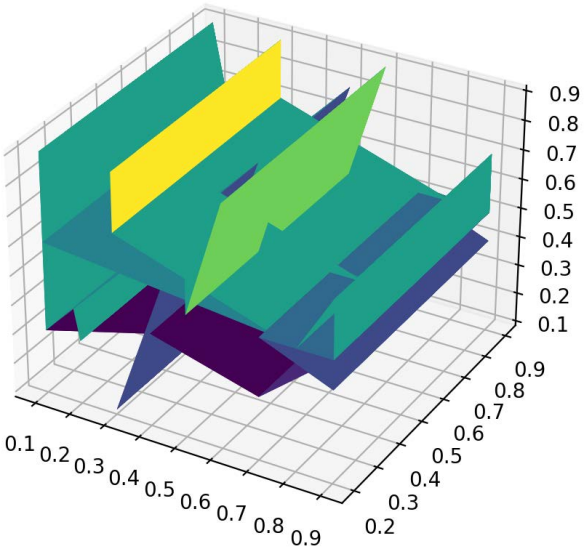

**FIGURE 3.** 3D surface plot of the macroscopic fuzzy evaluation system.

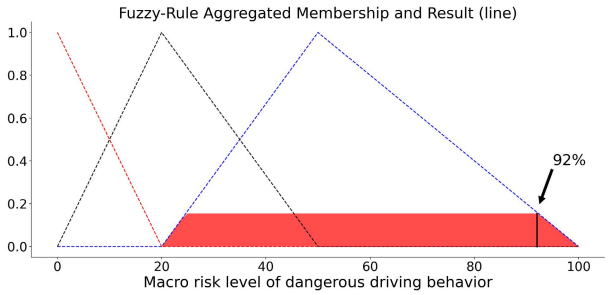


**FIGURE 4.** Use case of the macro driving behavior fuzzy inference system.

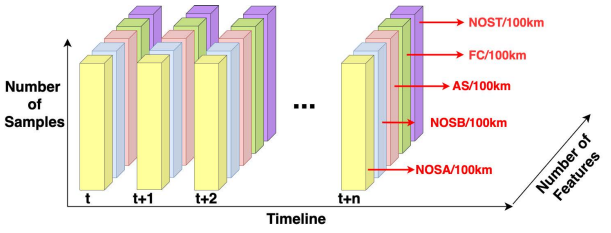


**FIGURE 5.** 3D matrix structure of driving behavior time-series data.

of the forget gate layer.

$$f_t = \varphi\left(W_f \times R_{level} \times \left[\mathbb{N}_{\text{seq}}, h_{t-1}\right] + b_f\right) \tag{10}$$

The input gate layer determines which driving behavior information is retained and uses the hyperbolic tangent activation function to calculate a vector to determine how much information is needed to update the current neural unit of the fuzzy-macro LSTM model. The input gate layer is implemented with (11) and (12), where $W_i$ is the weight matrix of the input gate layer, and $b_i$ is the deviation value of the input gate layer.

$$i_t = \varphi\left(W_i \times R_{level} \times \left[\mathbb{N}_{\text{seq}}, h_{t-1}\right] + b_i\right) \tag{11}$$

$$c_t = f_t \times c_{t-1} + i_t \times \tanh\left(W_t \times R_{level} \times \left[\mathbb{N}_{\text{seq}}, h_{t-1}\right] + b_c\right) \tag{12}$$

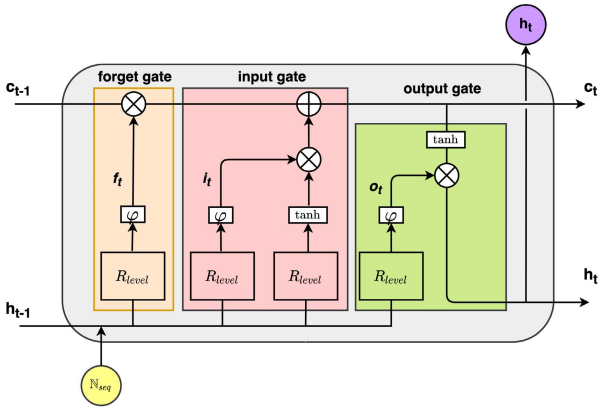


**FIGURE 6.** Neural unit structure of the fuzzy-macro LSTM model.

The output gate layer combines the calculation results of the forget and input gate layers to output the driving behavior information predicted by the current neural unit. The output gate performs data processing with (13) and (14). $W_o$ is the weight matrix of the output gate layer, and $b_o$ is the deviation value of the output gate layer.

$$o_t = \varphi\left(W_o \times R_{level} \times \left[\mathbb{N}_{\text{seq}}, h_{t-1}\right] + b_o\right) \tag{13}$$

$$h_t = o_t \times \tanh\left(c_t\right) \tag{14}$$

In our proposed fuzzy-macro LSTM, the dimension of the driving behavior input vector $\mathbb{N}_{\text{seq}}$ is $[29 \times 1]$. The output dimensionality is $[3 \times 1]$ and is the number of macro-risk classes. The dimensions of $h_t$, $h_{t-1}$, $c_t$, $c_{t-1}$, $i_t$, $o_t$, and $f_t$ are each $[3 \times 1]$, while the dimensions of the weight matrices $W_i$, $W_t$ and $W_o$ are each $[3 \times 29]$. The deviations $b_f$, $b_i$, $b_c$, and $b_o$ each have dimensions of $[3 \times 1]$.

## III. EXPERIMENTS AND RESULTS DISCUSSIONS

To evaluate the performance of our proposed fuzzy-macro LSTM model, we conduct a series of experiments and compare it with five other benchmark models. Our experiments are conducted on a Windows workstation with one NVIDIA Quadro P2200 GPU and 64 GB RAM. We implement the proposed fuzzy-macro LSTM approach in Python 3.8.2, Numpy 1.19.5 and Keras 2.4.3. We discuss the experimental environment, data set, and experimental result in the following sections.

### A. DATA SETS

In this study, a nonintrusive data collection method is used to collect the data of vehicles. We use an OBD-II adapter as the main data collection device because of its easy installation, strong data collection stability, low price, and high flexibility. Users can modify or add the driving behavior data fields they want to collect at any time in accordance with their needs. As shown in Figure 7, we install an OBD-II adapter on the experimenters' vehicles and continuously collect 9-month driving behavior data of 10 experimenters of different ages and genders. We install an app on the experimental drivers' smartphones to record the OBD-II adapter data via Bluetooth

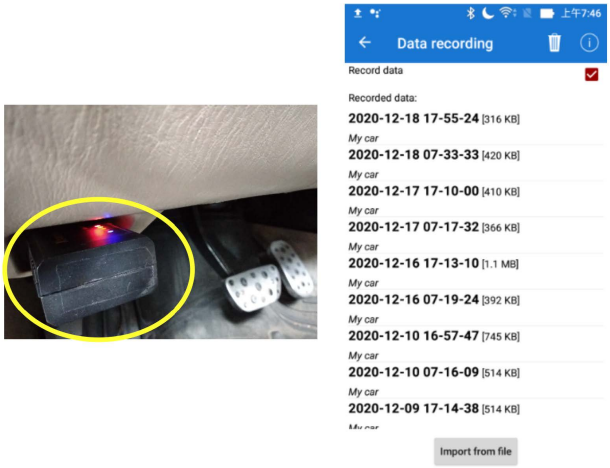


**FIGURE 7.** Data collection device and software. (a) OBD-II adapter mounted on the cars, (b) screenshot of the data-recording app.

and retransmit the data to a back-end cloud computing system via a 4G/5G telecommunication network. The collected driving behavior data consist of time, vehicle speed, average vehicle speed, travel distance, accumulated travel distance, engine coolant temperature, engine speed, and vehicle speed acceleration. Figure 8 shows a snippet of the sample dataset.

Before training the deep learning model, we use Python scikit-learn MinMaxScaler to rescale the data feature values to the range between 0 and 1. In addition, we use Python scikit-learn StandardScaler to standardize the data, which transforms the feature values to a Gaussian distribution, where the mean is 0 and the standard deviation is 1. We also use data engineering technology to generate more detailed driving behavior data, such as maximum vehicle speed, minimum vehicle speed, maximum engine revolutions per minute (RPM), and minimum RPM.

### B. EVALUATION METRICS

We compare the designed fuzzy-macro LSTM model with five other neural network models for time-series forecasts, namely, convolutional neural network (CNN), multilayer perceptron (MLP), Vanilla LSTM, CNN-LSTM, and ConvLSTM. The architectures of the five models are described as follows:

- CNN [21]: It is a 1D CNN that contains a convolutional hidden layer, a pooling layer, a flatten layer, and a dense layer.
- MLP [22]: It is an MLP neural network that has one neural hidden layer and one output layer.
- Vanilla LSTM: It is a variant of the LSTM neural network [16] and has a hidden layer of LSTM neural units and an output layer.
- CNN-LSTM [23]: It is a neural network that combines the CNN model with the LSTM model. The front end of the model is a 1D CNN that contains two convolutional hidden layers, a pooling layer, and a flatten layer.

| SECONDS | PID | VALUE | UNITS |
|---|---|---|---|
| 58433,40538 | OBD Module Voltage | 13,5 | V |
| 58434,59638 | Calculated engine load value | 22,74509804 | % |
| 58434,97438 | Engine coolant temperature | 88 | |
| 58435,35138 | Short term fuel % trim - Bank 1 | -0,78125 | % |
| 58435,73138 | Long term fuel % trim - Bank 1 | -11,71875 | % |
| 58436,11738 | Engine RPM | 899 | rpm |
| 58436,48538 | Vehicle speed | 88 | km/h |
| 58436,86438 | Timing advance | 14 | |
| 58437,24238 | Intake air temperature | 58 | |
| 58437,61838 | Calculated boost | -0,642772102 | bar |
| 58437,61838 | MAF air flow rate | 3,68 | g/sec |
| 58438,00238 | Fuel economizer (based on fuel system status and throttle position) | 1 | |
| 58438,00238 | Throttle position | 12,54901961 | % |
| 58438,38538 | Oxygen sensor 1 Bank 1 Short term fuel trim | 2,34375 | % |
| 58438,38538 | Oxygen sensor 1 Bank 1 Voltage | 0,325 | V |
| 58442,70238 | Average speed | 16,19231323 | km/h |
| 58443,11538 | Distance travelled | 2,305309863 | km |
| 58443,37538 | Distance travelled (total) | 2,305309863 | km |

**FIGURE 8.** Snippet of the sample data set.

The output of the CNN model is used as the input of the back-end LSTM model. The LSTM model contains an LSTM hidden layer and an output layer.

- ConvLSTM [24]: It is an RNN that has a 2D convolutional LSTM input layer, a flatten layer, a dense layer, and an output layer.

We use three major performance metrics to evaluate and compare model prediction performance, namely, mean absolute error (MAE), mean squared error (MSE), and root MSE (RMSE). The calculation of MAE is shown in (15), where $y_i$ is the true value and $\tilde{y}_i$ is the predicted value. MAE shows the average error between the actual macro dangerous driving degree and the predicted value. MSE is the mean of the sum of squared errors of the predicted macro dangerous driving degree and the corresponding points of the actual value, which is defined in (16). RMSE is calculated by (17). It is used to measure the deviation between the predicted value and the true value. In the above three model evaluation metrics, when the prediction error is large, the values of MAE, MSE, and RMSE are also large.

$$\text{MAE} = \frac{1}{N}\sum_{i=1}^{N}|y_i - \tilde{y}_i| \tag{15}$$

$$\text{MSE} = \frac{1}{N}\sum_{i=1}^{N}(y_i - \tilde{y}_i)^2 \tag{16}$$

$$\text{RMSE} = \sqrt{\frac{1}{N}\sum_{i=1}^{N}(y_i - \tilde{y}_i)^2} \tag{17}$$

### C. EXPERIMENT RESULTS

We compare the prediction performance of the fuzzy-macro LSTM model and the benchmark models in different training sample sizes and epochs. We evaluate the performance of all models when the training sample size is 1000 to 10000 and the number of training epochs is 50 to 500. Table 2 presents the comparison result for the impact of the number of training samples on performance. Table 3 shows the comparison result for the impact of the number of training epochs on performance. We also present the data analysis results of drivers' macro dangerous driving behaviors and verify the concept of macroscopic data analysis of driving behaviors proposed in this study.

#### 1) MACROSCOPIC RISK LEVEL ANALYSIS

Before training the model, we analyze the importance of various features of driving behaviors and vehicle conditions on the predicted macroscopic dangerous driving behaviors. Figure 9 presents the SHapley Additive exPlanations (SHAP) summary plot showing the contribution of each feature to the predicted degree of macro dangerous driving behavior. SHAP values are based on game theory to evaluate the degree of influence of all features on the predicted features in a fair manner [25]. Figure 9 presents the importance of 10 features to the predicted degree of macro dangerous driving from high to low. Among the 10 features, 6 are related to vehicle condition data, and 4 are related to driving behavior data. The top three driving behavior features that have the greatest impact on the predicted degree of macroscopic dangerous driving behavior are the numbers of sudden braking per 100 km, the numbers of sudden accelerations per 100 km, and the average speed per 100 km. This analysis result is consistent with the three driving behavior factors in the macroscopic dangerous driving behavior fuzzy inference system designed in Section II.

We further analyze the changes in the degree of macroscopic dangerous driving of experimental drivers. As shown in Figure 10, the macroscopic risky driving degree of three drivers varies in different periods. Among them, Driver 3 had the highest degree of dangerous driving from October to December 2020. Driver 1 had the lowest risk degree of dangerous driving in October and November 2020 and the highest risk of dangerous driving in December 2020. Driver 2 had the highest risk of dangerous driving in November 2020. In December 2020, his dangerous driving behavior improved, and the risk level was reduced. The analysis results in Figure 10 verify the effectiveness of our proposed concepts of macroscopically, dynamically, and adaptively evaluating drivers' dangerous driving behaviors.

#### 2) PERFORMANCE ANALYSIS OF MAE

Figures 11 and 12 compare the performance of the fuzzy-macro LSTM model and the five other time-series forecasting models in MAE. The box-and-whisker plot in Figure 11 presents the analysis results of the impact of the number of training samples on the MAE performance of various models. Fuzzy-macro LSTM has the smallest average value of MAE and the best overall performance. The average MAE of the ConvLSTM model is 0.845, and that of the fuzzy-macro LSTM model is 0.612. Compared with the ConvLSTM model, the fuzzy-macro LSTM model reduces the MAE of the prediction error by nearly 27.62%. Figure 12 shows the results of the analysis of the impact of the number of training epochs on the performance of various models in MAE. The fuzzy-macro LSTM has stable MAE changes in different epochs and achieves the lowest value. The CNN and MLP models can maintain relatively low MAE values when the number of training epochs is less than 200. When the number of training epochs exceeds 200, the MAE values

**TABLE 2.** Comparison of the impact of training sample size on performance for predicting macro risk level.

| Metrics | Method | Samples | | | | | | | | | |
|---|---|---|---|---|---|---|---|---|---|---|---|
| | | 1000 | 2000 | 3000 | 4000 | 5000 | 6000 | 7000 | 8000 | 9000 | 10000 |
| MAE | CNN | 0.700 | 0.728 | 0.713 | 0.723 | 0.715 | 0.722 | 0.709 | 0.716 | 0.699 | 0.702 |
| | MLP | 0.690 | 0.716 | 0.693 | 0.712 | 0.716 | 0.714 | 0.707 | 0.716 | 0.703 | 0.701 |
| | Vanilla LSTM | 0.667 | 0.677 | 0.682 | 0.685 | 0.689 | 0.687 | 0.687 | 0.691 | 0.688 | 0.688 |
| | CNN-LSTM | 0.803 | 0.810 | 0.795 | 0.801 | 0.784 | 0.777 | 0.757 | 0.743 | 0.733 | 0.726 |
| | ConvLSTM | 0.893 | 0.847 | 0.867 | 0.857 | 0.838 | 0.841 | 0.836 | 0.833 | 0.827 | 0.810 |
| | **fuzzy-macro LSTM** | **0.593** | **0.601** | **0.611** | **0.613** | **0.616** | **0.614** | **0.615** | **0.619** | **0.617** | **0.616** |
| MSE | CNN | 0.698 | 0.747 | 0.751 | 0.758 | 0.725 | 0.737 | 0.719 | 0.718 | 0.688 | 0.686 |
| | MLP | 0.686 | 0.720 | 0.687 | 0.712 | 0.730 | 0.712 | 0.701 | 0.725 | 0.695 | 0.670 |
| | Vanilla LSTM | 0.554 | 0.573 | 0.584 | 0.587 | 0.594 | 0.590 | 0.589 | 0.596 | 0.590 | 0.587 |
| | CNN-LSTM | 1.014 | 1.000 | 0.985 | 0.957 | 0.925 | 0.900 | 0.859 | 0.838 | 0.829 | 0.829 |
| | ConvLSTM | 1.197 | 1.109 | 1.169 | 1.096 | 1.071 | 1.061 | 1.041 | 1.035 | 1.031 | 0.974 |
| | **fuzzy-macro LSTM** | **0.493** | **0.499** | **0.502** | **0.506** | **0.511** | **0.509** | **0.507** | **0.510** | **0.509** | **0.506** |
| RMSE | CNN | 0.841 | 0.871 | 0.870 | 0.866 | 0.855 | 0.859 | 0.848 | 0.846 | 0.828 | 0.828 |
| | MLP | 0.816 | 0.847 | 0.830 | 0.843 | 0.854 | 0.844 | 0.838 | 0.847 | 0.835 | 0.822 |
| | Vanilla LSTM | 0.745 | 0.757 | 0.764 | 0.768 | 0.770 | 0.769 | 0.769 | 0.772 | 0.768 | 0.766 |
| | CNN-LSTM | 0.966 | 1.002 | 0.982 | 0.981 | 0.956 | 0.949 | 0.938 | 0.922 | 0.912 | 0.905 |
| | ConvLSTM | 1.093 | 1.048 | 1.072 | 1.046 | 1.025 | 1.032 | 1.025 | 1.012 | 1.017 | 0.998 |
| | **fuzzy-macro LSTM** | **0.691** | **0.696** | **0.699** | **0.707** | **0.708** | **0.706** | **0.704** | **0.707** | **0.707** | **0.706** |

**TABLE 3.** Comparison of the impact of training epochs on performance for predicting macro risk level.

| Metrics | Method | Epochs | | | | | | | | | |
|---|---|---|---|---|---|---|---|---|---|---|---|
| | | 50 | 100 | 150 | 200 | 250 | 300 | 350 | 400 | 450 | 500 |
| MAE | CNN | 0.694 | 0.715 | 0.743 | 0.770 | 0.799 | 0.824 | 0.849 | 0.866 | 0.889 | 0.895 |
| | MLP | 0.701 | 0.719 | 0.741 | 0.776 | 0.803 | 0.824 | 0.839 | 0.856 | 0.861 | 0.879 |
| | Vanilla LSTM | 0.689 | 0.687 | 0.687 | 0.687 | 0.688 | 0.688 | 0.689 | 0.688 | 0.689 | 0.693 |
| | CNN-LSTM | 0.787 | 0.846 | 0.806 | 0.785 | 0.773 | 0.757 | 0.750 | 0.737 | 0.734 | 0.732 |
| | ConvLSTM | 0.775 | 0.838 | 0.822 | 0.811 | 0.800 | 0.796 | 0.790 | 0.784 | 0.777 | 0.776 |
| | **fuzzy-macro LSTM** | **0.613** | **0.612** | **0.611** | **0.612** | **0.615** | **0.619** | **0.620** | **0.620** | **0.624** | **0.630** |
| MSE | CNN | 0.660 | 0.731 | 0.810 | 0.889 | 0.963 | 1.018 | 1.080 | 1.142 | 1.183 | 1.252 |
| | MLP | 0.656 | 0.740 | 0.819 | 0.906 | 0.976 | 1.039 | 1.088 | 1.130 | 1.163 | 1.187 |
| | Vanilla LSTM | 0.593 | 0.593 | 0.592 | 0.593 | 0.594 | 0.596 | 0.600 | 0.607 | 0.613 | 0.629 |
| | CNN-LSTM | 0.945 | 1.063 | 0.961 | 0.919 | 0.888 | 0.862 | 0.842 | 0.826 | 0.819 | 0.815 |
| | ConvLSTM | 0.911 | 1.085 | 1.023 | 0.987 | 0.952 | 0.939 | 0.924 | 0.915 | 0.904 | 0.889 |
| | **fuzzy-macro LSTM** | **0.521** | **0.520** | **0.521** | **0.521** | **0.523** | **0.525** | **0.531** | **0.533** | **0.535** | **0.540** |
| RMSE | CNN | 0.805 | 0.858 | 0.902 | 0.938 | 0.984 | 1.015 | 1.046 | 1.066 | 1.086 | 1.118 |
| | MLP | 0.808 | 0.855 | 0.908 | 0.951 | 0.991 | 1.021 | 1.048 | 1.064 | 1.075 | 1.090 |
| | Vanilla LSTM | 0.770 | 0.770 | 0.769 | 0.770 | 0.770 | 0.772 | 0.774 | 0.778 | 0.781 | 0.792 |
| | CNN-LSTM | 0.976 | 1.026 | 0.981 | 0.961 | 0.946 | 0.923 | 0.919 | 0.909 | 0.903 | 0.897 |
| | ConvLSTM | 0.944 | 1.028 | 1.013 | 0.995 | 0.980 | 0.969 | 0.959 | 0.956 | 0.951 | 0.949 |
| | **fuzzy-macro LSTM** | **0.733** | **0.731** | **0.730** | **0.731** | **0.732** | **0.734** | **0.736** | **0.737** | **0.740** | **0.744** |

predicted by the CNN and MLP models gradually increase. When the number of training epochs is 500, the MAE of the fuzzy-macro LSTM model is 0.630 and that of the CNN model is 0.895, indicating that the fuzzy-macro LSTM model achieved a 29.61% improvement in MAE compared with the CNN model. Figure 13 compares the overall MAE performance of all models in different numbers of training samples and epochs. The experimental results show that compared with the five other time-series forecasting models, the fuzzy-macro LSTM model has the smallest forecasted MAE error when the number of training samples and epochs change, and its overall performance is the best.

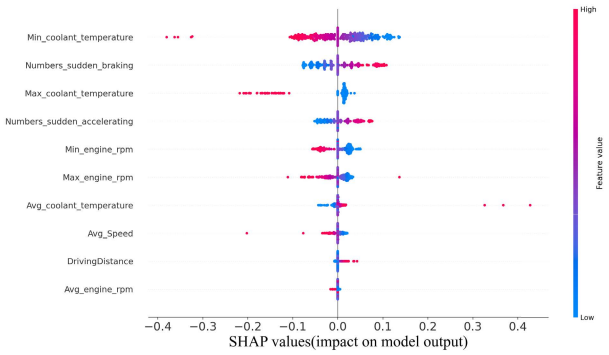


**FIGURE 9.** Feature importance analysis with SHAP values.

### 3) PERFORMANCE ANALYSIS OF MSE

Figures 14 and 15 depict the comparison results for the fuzzy-macro LSTM model and the five other time-series forecasting models in MSE performance. Figure 14 presents the analysis results of the impact of the number of training samples on the performance of various models in MSE. The fuzzy-macro LSTM has the lowest average MSE value of 0.505 and the smallest average prediction error. By contrast, the ConvLSTM model has the highest average MSE value of 1.078 and the largest average prediction error. Compared with the ConvLSTM model, the fuzzy-macro LSTM model reduces the MSE of the prediction error by nearly 53.16%. Figure 15 presents the analysis results of the impact of the

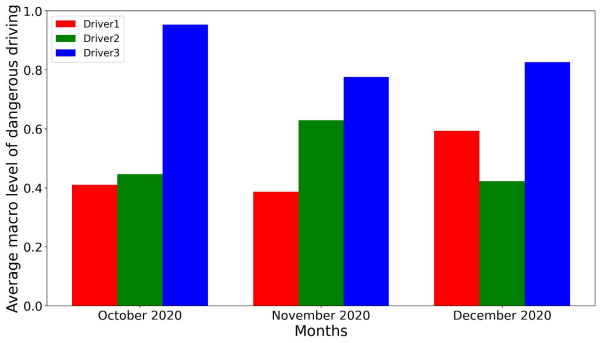


**FIGURE 10.** Drivers' macroscopic dangerous driving degree analysis.

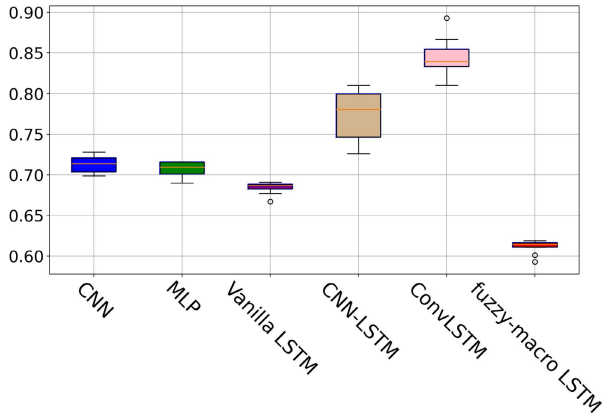


**FIGURE 11.** Comparison of the impact of training sample size on MAE.

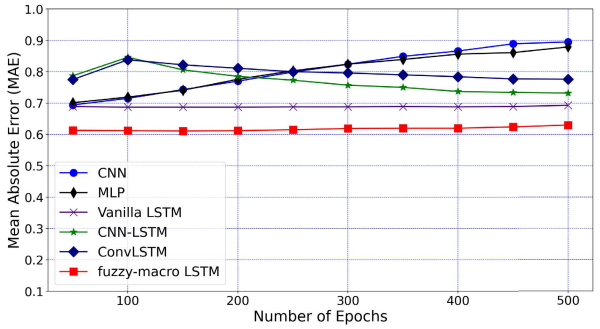


**FIGURE 12.** Comparison of the impact of training epoch size on MAE.

number of training epochs on the performance of various models in MSE. As the number of epochs changes, the MSE change of fuzzy-macro LSTM is relatively stable and has the lowest value. The MSE performance of CNN and MLP models is similar to that of their MAE. CNN and MLP models can maintain a low MSE when the number of training epochs is less than 200. However, when the number of training epochs exceeds 200, the value of MSE predicted by CNN and MLP models increases significantly. When the number of training epochs is 500, the MSE of the fuzzy-macro LSTM model is 0.540, the MAE of the CNN model is 1.252, and the fuzzy-macro LSTM model improves MSE by 56.87% compared with the CNN model.

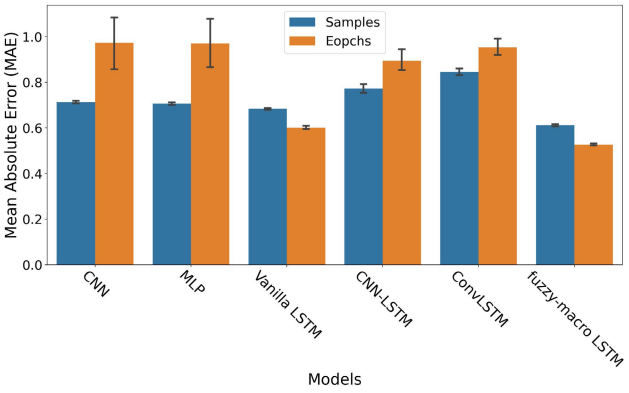


**FIGURE 13.** Comparison of the impact of training samples and epochs on MAE.

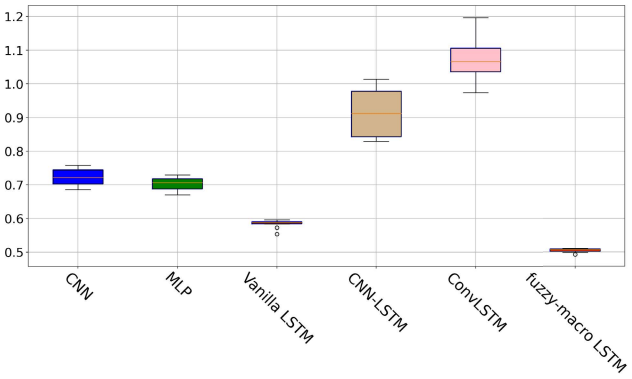


**FIGURE 14.** Comparison of the impact of training sample size on MSE.

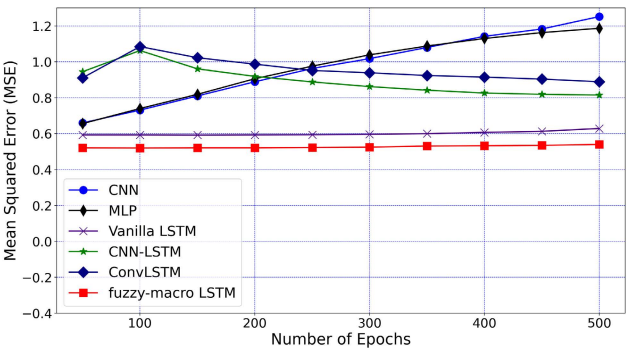


**FIGURE 15.** Comparison of the impact of training epoch size on MSE.

Figure 16 compares the overall impact of the number of training samples and epochs on the MSE of all models. The experimental results show that compared with the five other time-series forecasting models, the fuzzy-macro LSTM model predicts the smallest MSE error and has the best overall performance is the best. For CNN and MLP models, when the number of training epochs changes, their average MSE errors are higher than those of the other models. The ConvLSTM model has the largest average MSE and the highest prediction error when the number of training samples changes. These phenomena also verify the experimental results in Figures 14 and 15.

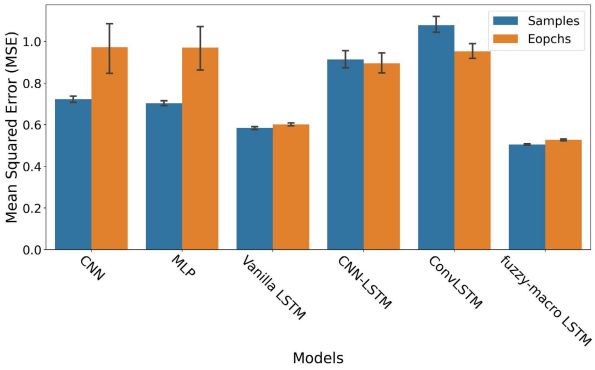


**FIGURE 16.** Comparison of the impact of training samples and epochs on MSE.

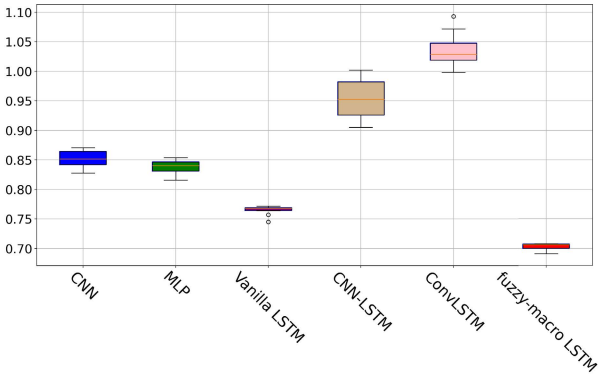


**FIGURE 17.** Comparison of the impact of training sample size on RMSE.

### 4) PERFORMANCE ANALYSIS OF RMSE

Figures 17 and 18 show the RMSE performance comparison results for the fuzzy-macro LSTM model and the five other time-series forecasting models. Figure 17 shows the analysis results of the impact of the number of training samples on the RMSE of various models. Given that the calculation of RMSE is the root of MSE, similar to the experimental results in Figure 14, fuzzy-macro LSTM has an average RMSE value of 0.703 and the smallest prediction error. The average RMSE of the ConvLSTM model is 1.041, and its prediction error is the largest.

Figure 18 presents the analysis results of the impact of the number of training epochs on the RMSE performance of various models. As the number of epochs changes, the RMSE of fuzzy-macro LSTM is relatively stable and has the lowest value. The RMSE changes of CNN and MLP models are similar to the changes in their MAE and MSE. When the number of training epochs reaches 500, the RMSE of the CNN model has the largest value, which is 1.118, whereas the RMSE of the fuzzy-macro LSTM model is only 0.744. Compared with the CNN model, the fuzzy-macro LSTM model reduces the prediction error of RMSE by 33.45%.

Figure 19 compares the overall impact of the number of training samples and epochs on the RMSE of all models. The experimental results show that compared with the five other time-series forecasting models, the fuzzy-macro LSTM model can maintain the smallest prediction error when the

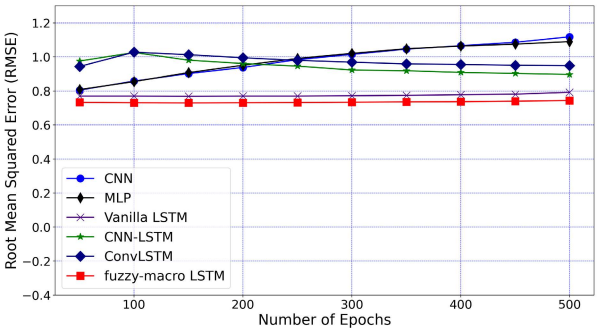


**FIGURE 18.** Comparison of the impact of the number of training epochs on RMSE.

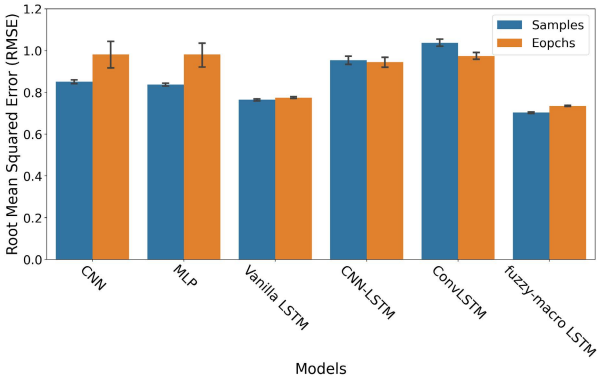


**FIGURE 19.** Comparison of the impact of training samples and epochs on RMSE.

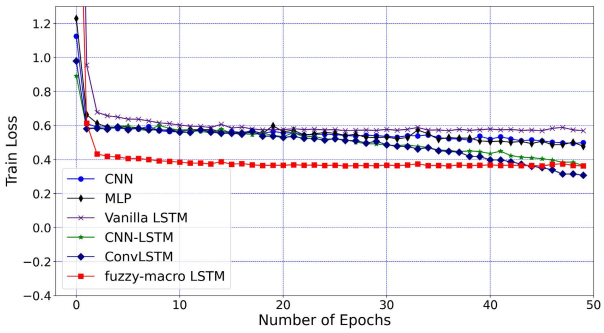


**FIGURE 20.** Comparison of training loss on predicting macro risk level.

numbers of training samples and epochs change, and its overall performance is the best. When the number of training epochs changes for CNN and MLP models, their average prediction errors increase. The ConvLSTM model has the largest average RMSE and the highest prediction error with the change in training samples. These observations verify the experimental results in Figures 17 and 18.

To show a more complete analysis result, this research refers to the experimental analysis method of [26] and analyzes the predicted performance in depth from the perspective of overall performance analysis. Table 4 presents the overall performance comparison of predicting various driving behaviors with different methods. The experimental results in Table 4 indicate that the fuzzy-macro LSTM model has the best prediction accuracy when predicting various driving

**TABLE 4. Overall comparison of performance for predicting various driving behaviors.**

| Method | Fast Acceleration | | | | Hard Braking | | | | Average Speed | | | | Macro Risk Level | | | |
|---|---|---|---|---|---|---|---|---|---|---|---|---|---|---|---|---|
| | MAE | RMSE | MSE | Training Time (hrs:mins:sec) | MAE | RMSE | MSE | Training Time (hrs:mins:sec) | MAE | RMSE | MSE | Training Time (hrs:mins:sec) | MAE | RMSE | MSE | Training Time (hrs:mins:sec) |
| MLP | 5.397 | 6.655 | 44.225 | 0:57:37 | 4.583 | 5.735 | 32.876 | 0:54:11 | 5.762 | 10.597 | 114.159 | 0:55:01 | 0.701 | 0.808 | 0.656 | 0:48:10 |
| CNN | 5.468 | 6.670 | 44.629 | 3:08:29 | 4.506 | 5.565 | 31.061 | 3:08:42 | 5.891 | 10.752 | 114.979 | 3:05:48 | 0.694 | 0.805 | 0.660 | 3:11:27 |
| Vanilla LSTM | 4.796 | 5.780 | 33.219 | 2:22:01 | 3.888 | 4.781 | 22.919 | 2:26:31 | 5.376 | 10.477 | 107.981 | 2:23:06 | 0.689 | 0.770 | 0.593 | 2:01:19 |
| CNN-LSTM | 5.649 | 6.944 | 48.631 | 3:43:39 | 4.522 | 5.769 | 33.026 | 3:44:45 | 6.275 | 11.385 | 132.756 | 3:43:31 | 0.787 | 0.976 | 0.945 | 3:42:24 |
| ConvLSTM | 5.756 | 7.140 | 51.200 | 5:26:42 | 4.669 | 5.929 | 35.091 | 5:31:19 | 7.032 | 11.936 | 140.916 | 5:27:26 | 0.775 | 0.944 | 0.911 | 5:22:05 |
| **fuzzy-macro LSTM** | **4.235** | **5.451** | **31.326** | **1:47:07** | **3.515** | **4.595** | **22.025** | **1:51:28** | **4.726** | **9.959** | **102.647** | **1:45:19** | **0.613** | **0.733** | **0.521** | **1:23:16** |

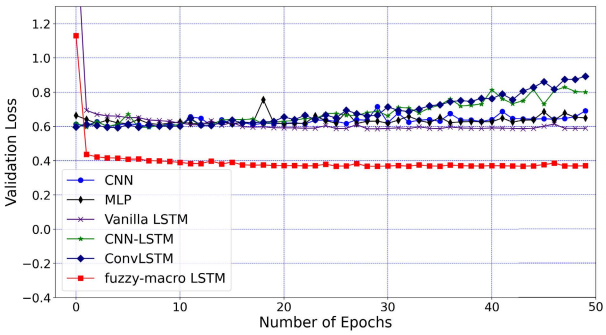


**FIGURE 21. Comparison of validation loss on predicting macro risk level.**

behaviors of drivers, including the number of sudden acceleration, the number of sudden braking, and the average vehicle speed, compared with other methods. When predicting the number of sudden accelerations, the fuzzy-macro LSTM model achieved MAE, RMSE, and MSE of 4.235, 5.451, and 31.326, respectively. Compared with the ConvLSTM model, the fuzzy-macro LSTM model improved the performance of predicting sudden acceleration by an average of 29.68%. When predicting the number of sudden braking, the fuzzy-macro LSTM model achieved MAE, RMSE, and MSE of 3.515, 4.595, and 22.025, respectively. Compared with the ConvLSTM model, the fuzzy model improved the predicted sudden braking performance by up to 37.23% (MSE). When the average speed of the driver was predicted, the MAE, RMSE, and MSE of the fuzzy-macro LSTM model were 7.032, 11.936, and 140.916, respectively. Compared with the ConvLSTM model, the fuzzy model improved the performance of predicting the average speed by up to 32.79% (MAE). The fuzzy-macro LSTM model performed best in predicting various specific driving behaviors. Therefore, it is also expected to perform best in predicting the overall macro risk level. The MAE, RMSE, and MSE of the fuzzy-macro LSTM model were 0.613, 0.733, and 0.521, respectively. Compared with the CNN-LSTM model, the fuzzy model improved the performance of predicting the macroscopic risk level of drivers' dangerous driving by up to 44.87% (MSE). With regard to the training time of the model, because the structure of the neural network of MLP is not as complicated as that of the other models, the MLP has the shortest training time, but its prediction accuracy is not good. ConvLSTM has the longest training time due to its complex network architecture and learning mechanism. The proposed fuzzy-macro LSTM model has a shorter training time, saving an average of 68.91% of the training time compared with the ConvLSTM network, and it can improve the overall prediction accuracy by an average of 30.1%.

Training learning curve gives an idea of how well the model is learning, and validation learning curve gives an idea of how well the model is generalizing. Figures 20 and 21 show the training and validation loss curves, respectively, for all models when they are trained to predict the macroscopic risk levels of drivers. The x-axis of Figures 20 and 21 is the number of epochs during the training. The vertical axis of Figure 20 is the training loss value, and that of Figure 21 is the validation loss value. From Figures 20 and 21, we observe that the fuzzy-macro LSTM model and other models, except for the CNN-LSTM and ConvLSTM models, can show a convergence trend as the number of training epochs increases. The CNN-LSTM model and the ConvLSTM model suffer from overfitting as the number of epochs increases. Compared with other models, the training loss curve and validation loss curve of the fuzzy-macro LSTM model have the most stable changes. The fuzzy-macro LSTM model is identified as a well-fitting predictive model by the training and validation losses as the gap between the stable points of the training and validation loss values is kept to a minimum.

### 5) PERFORMANCE ANALYSIS OF MULTISTEP PREDICTIONS

To verify the functional effectiveness of the fuzzy-macro LSTM model we designed for predicting drivers' future dangerous driving behaviors, we conduct experiments to predict three driving behaviors and compare the predicted results with actual driving behaviors. Figures 22 to 24 present the experimental results. Figure 22 shows a comparison of our predicted average vehicle speed of test driver no. 2 for the next 10 days and the average vehicle speed while driving. Figure 23 depicts a comparison of the number of sudden braking that we predicted for test driver no. 2 in the next 20 days and the actual values while driving. Figure 24 demonstrates a comparison between the number of sudden accelerations that we predicted for test driver no. 2 in the next 30 days and the real sudden accelerations during driving. The results of the three experiments show that the driving behavior predicted by the fuzzy-macro LSTM model is considerably close to the real driving behavior. Therefore, fuzzy-macro LSTM can accurately predict a driver's future dangerous driving behavior.

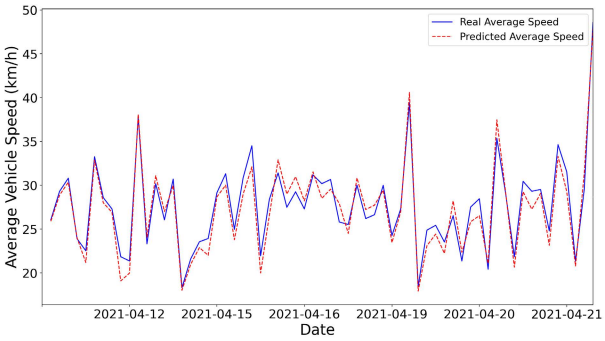


**FIGURE 22.** Predicted 10-day average vehicle speed.

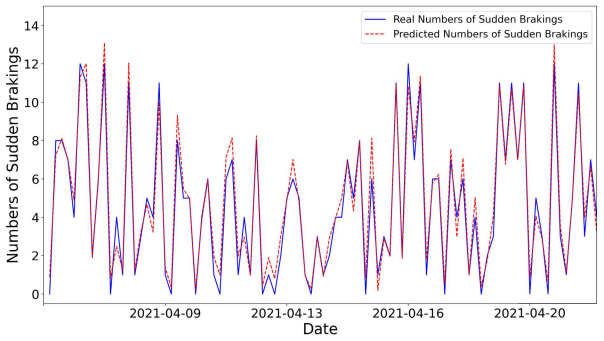


**FIGURE 23.** Predicted 20-day sudden braking.

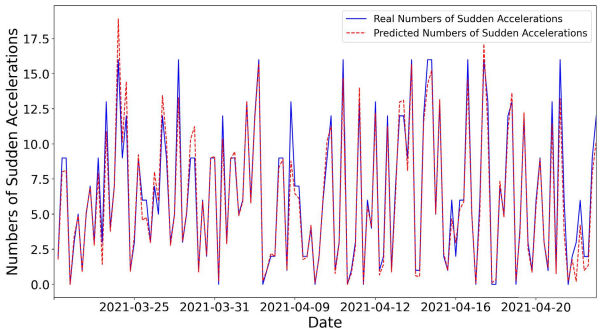


**FIGURE 24.** Predicted 30-day sudden accelerations.

## IV. BACKGROUND AND RELATED WORKS

Detecting and analyzing driving behavior have long been an important research topic and an active research field [27]–[29]. The methodology for driving behavior analysis and detection in the existing literature is mainly divided into two types: real-time and non-real-time driving behavior analysis and detection. The analyzed and detected driving behavior mainly includes fatigued driving, distracted driving, dangerous driving, and drunk driving [30]. Table 5 presents an overview of driving behavior detection and analysis approaches.

Many studies [8], [31]–[33] required the use of special devices, such as cameras, and biological signal sensing. Certain dangerous driving behaviors (such as distracted driving and fatigued driving) can be detected by special algorithms. Some studies [8], [33] used drivers' smartphones as sensing devices. Various algorithms and models have been designed

**TABLE 5.** Overview of driving behavior detection and analysis approaches.

| Approaches | Driving Behaviors | Types | Data Collection Devices |
|---|---|---|---|
| Computer Vision and Image Processing | fatigued driving [31], [32], dangerous driving [8], [33] | real-time non-real-time | dashboard-mounted camera, smartphone |
| Kalman Filter | fatigued driving [34], dangerous driving [7], [35] | real-time, non-real-time | camera, OBD-II adaptor |
| Hidden Markov Model | dangerous lane change [36], fatigued driving [11], dangerous corner driving [37] | real-time, non-real-time | data simulator, wearable sensor, GPS tracker |
| Statistical Probability Model | drunk driving [12], reckless driving [12], fatigued driving [12], dangerous driving [13] | non-real-time | GPS tracker, speed sensor, eye camera, lane camera, accelerometer sensor, alcohol sensor, video camera, 3D acceleration sensor, speech and noise sensor, heart rate sensor, laser scanner, pedal pressure senor, steering angle sensor, skin conductance sensor |
| Fuzzy Logics | dangerous driving [38], distracted driving [39] | real-time, non-real-time | smartphone |
| Neuro-Fuzzy Network | fatigued driving [40], distracted driving [41] | non-real-time | smartphone, steering angle sensor |
| Deep Learning Model | fatigued driving [6], distracted driving [8], [42] | non-real-time | digital video recording camera, dash camera, OBD-II adaptor |

to analyze data sensed by the built-in camera and sensor on a driver's smartphone. Dangerous behaviors, such as distracted driving and drowsy driving, may be detected and identified. However, the placement of drivers' smartphones in vehicles has a dramatic impact on the accuracy of collected data, which can severely affect the accuracy of detecting and analyzing driving behavior.

Research [7], [34], [35] detected driving behavior on the basis of the Kalman filter. Kłusek *et al.* [7] trained an LSTM network model to predict driving-related signals, such as vehicle speed or acceleration. Before training the model, they used the Kalman filter to preprocess collected data to eliminate uncertain noise and achieve a well-trained linear evaluation model. Hwang *et al.* [35] designed an analysis method based on driving behavior data collected using OBD. They applied the Kalman filter to organize and clean the data to reduce the abnormal data of the samples. The authors trained a random forest machine learning model to classify drivers for dangerous driving, which can distinguish three kinds of dangerous driving behaviors.

A hidden Markov model (HMM) is a well-known statistical model that describes unknown hidden parameters. It is widely used in speech recognition, bioinformatics, time-series analysis, and driving behavior analysis. In [11], various wearable sensors were affixed to a driver to collect signals, such as electroencephalogram, electromyography, and respiratory signal data, and an HMM was designed to monitor the fatigued driving degree of drivers dynamically. In [36], an HMM-based method was proposed to detect three driving behaviors: emergency lane change, normal lane change, and lane maintenance. This article used simulation to verify whether the designed method can effectively identify the three driving behaviors during changing lanes. Yao *et al.* [37] installed GPS trackers on some experimenters' vehicles to collect driving behavior data and chose vehicle speed, acceleration, yaw rate, and sideslip angle in the experimental data as clustering indicators. The clustering results were sent to an HMM to detect the behavioral characteristics of drivers when they were turning the vehicles.

Some studies analyzed various collected sensor data on the basis of probability statistical models. Al-Sultan *et al.* [12] designed a five-layer perception system architecture to collect and analyze data, such as vehicle speed, alcohol sensor data, lane sensor data, gravity acceleration sensor data, and GPS sensor data. They also designed a probabilistic model based on dynamic Bayesian networks. The model can infer four driving behaviors by combining contextual data related to the driver, vehicle, and driving environment; these behaviors are normal driving, drunk driving, reckless driving, and fatigued driving. Miyajima and Takeda [13] installed up to 10 sensing devices on a vehicle, including heartbeat sensors, skin conductance sensors, pedal sensors, and video recorders, to collect various sensing data and designed a Gaussian mixture model that detects the driver's driving behaviors. Their model can infer drivers' dangerous driving behavior through analyzing various driving behaviors, such as pedal operation, car-following, and lane changing.

Driving behavior detection based on fuzzy theory is also one of the main research methods. The SenseFleet platform was designed in [38] to collect and analyze a driver's smartphone data. The core of the platform is a fuzzy logic calculation system that can calculate the safe driving scores of different drivers. Nonetheless, the SenseFleet platform is mainly used to analyze a driver's past dangerous driving behavior. It cannot assess the driver's comprehensive dangerous behavior level nor can it predict the driver's possible future dangerous driving behavior and degree of danger. Aksjonov *et al.* [39] designed system architecture and methods to analyze and evaluate drivers' driving attention. A fuzzy logic algorithm was designed to evaluate the performance of a driver in remaining in their lane and the vehicle speed when driving the car in specific road sections to analyze the driver's degree of distracted driving. Some research also used neuro-fuzzy systems to judge driving behavior. Eftekhari and Ghatee [40] proposed a neuro-fuzzy system that collects the acceleration sensor data from a driver's smartphone to analyze the driver's driving behavior of changing lanes, turning, and turning around. They designed fuzzy calculation logic to evaluate whether the driver is performing safe driving or reckless driving. However, the placement of the mobile phone may affect the accuracy of inference. Arefnezhad *et al.* [41] designed a driver's drowsiness detection system based on the driver's steering wheel data. The system is a self-adjusting neuro-fuzzy inference system that contains a feature data selector to select the features that are most relevant to the level of drowsiness and to detect whether the driver is sleepy or awake.

With the rise of big data and machine learning technology, some studies [6], [8], [42] have utilized deep learning to solve the problem of how to detect and analyze driving behavior. In [6], Shahverdy *et al.* designed a method to detect and classify driving behavior by using a CNN. They collected driving behavior data, including vehicle speed, acceleration, gravitational acceleration, vehicle speed, and rotational speed. The data were then processed as the input of the CNN to train the CNN model, such that the model can automatically judge the driving behavior of drivers. The authors stated that their method can effectively distinguish five driving behaviors, namely, normal, aggressive, distracted, drowsy, and drunk driving. However, this study did not discuss how the future driving behavior of drivers can be predicted. Huang *et al.* designed a hybrid CNN framework to analyze and classify photos of various driving behaviors [8]. This research integrated ResNet50, Inception V3, and Xception models to design a cooperative pretrained model and then reconnected and sent the output of the pretrained model to a full-link CNN for training. The trained model can classify driving behavior photos and distinguish nine types of distracted driving behaviors. This study mainly aimed to train a complex variant of CNN to identify various driving behavior images.

Existing research methods mainly use various sensing devices and algorithms to classify driving behavior. Research has focused on analyzing single or multiple driving behaviors that have occurred. Few studies have assessed the overall risk of driving behavior and predicted future driving behavior. The difference between this research and related work is that we use fuzzy theory to analyze dangerous driving behavior comprehensively and evaluate the degree of danger of all drivers from a macro perspective. In addition, we propose a novel time-series forecasting deep learning model to predict dangerous driving behaviors. The proposed method can be provided to industries, such as fleet management and car insurance companies, as a reference for risk reduction and accident prevention.

## V. CONCLUSION AND FUTURE WORKS

This paper proposes a method to analyze and predict dangerous driving behavior on IoV from a macro perspective. We summarize important research methods in the field of driving behavior detection and analysis, and we discuss the main characteristics of various methods. Although many driving behavior analysis systems and methods have been

designed with the development of technology, objective and cost-effective driving behavior analysis and prediction solutions for the public drivers of ordinary vehicles are still lacking. This research aims to address this issue.

We adopt three important macro driving behaviors, namely, the number of sudden braking per 100 km, the number of sudden acceleration per 100 km, and the average speed per 100 km, as the reference factors for designing a fuzzy inference macroscopic dangerous driving behavior degree system. System users can flexibly adjust the reference factors and choose their preferred dangerous driving behaviors, such as the number of instances of speeding, the number of instances of drunk driving, the number of sharp turns, and the length of driving time. With the varied and complicated driving behavior patterns of drivers in different regions and age–gender groups, users can select the most appropriate macro risk driving behavior factors in accordance with a specific gender or age group. They can then use the fuzzy inference system of this research to evaluate the risk level of dangerous driving behavior for all drivers.

We also design a fuzzy-macro LSTM model, which is based on an RNN to strengthen the memory on drivers' driving habits and the degree of dangerous driving behavior, learn driving behavior patterns, and predict dangerous driving behaviors. The experimental results verify that the proposed method can achieve a macroscopic analysis of the degree of dangerous driving of all drivers. In addition, compared with five other neural network models for time-series prediction, the fuzzy-macro LSTM model has the smallest prediction error.

Auto property insurance companies or fleet management users could analyze high-risk drivers promptly by using the systems and models designed in this research. The data analysis and prediction results could be used as a reference for improving other applications, such as driving behavior monitoring and alert, accident prevention, and damage prevention. Given the diverse and complex driving behaviors, determining how to apply our proposed method to detect more complex driving behaviors is one of our future works. Recently, attention and transformer-based models have shown great power in unified modeling, with the transformer model achieving excellent results on many prediction tasks in natural language processing. The application of transformer to time-series forecasting problems has also attracted the interest of many researchers [43]. In the future, we will also study how the attention and transformer-based model can be used to predict various dangerous driving behaviors on the IoV from the level of adding position encoding and optimizing the attention module. Another future subject for in-depth research is how our designed fuzzy inference macroscopic dangerous driving degree system can be optimized. The concepts of macro analysis and prediction of driving behavior proposed in this research will also be implemented on IoV service providers and IoV platforms to complete proof of service.

## ACKNOWLEDGMENT

The authors would like to thank the reviewers for their constructive comments and suggestions to improve the quality of this article.

## REFERENCES

[1] F. Yang, J. Li, T. Lei, and S. Wang, "Architecture and key technologies for internet of vehicles: A survey," *J. Commun. Inf. Netw.*, vol. 2, no. 2, pp. 1–17, Jun. 2017.

[2] R. Hao, H. Yang, and Z. Zhou, "Driving behavior evaluation model base on big data from internet of vehicles," *Int. J. Ambient Comput. Intell.*, vol. 10, no. 4, pp. 78–95, 2019.

[3] D. C. Li, L.-D. Chou, L.-M. Tseng, Y.-M. Chen, and K.-W. Kuo, "A bipolar traffic density awareness routing protocol for vehicular ad hoc networks," *Mobile Inf. Syst.*, vol. 2015, pp. 1–12, Sep. 2015.

[4] K. N. Qureshi, S. Din, G. Jeon, and F. Piccialli, "Internet of vehicles: Key technologies, network model, solutions and challenges with future aspects," *IEEE Trans. Intell. Transp. Syst.*, vol. 22, no. 3, pp. 1777–1786, Mar. 2021.

[5] D. C. Li, B.-H. Chen, C.-W. Tseng, and L.-D. Chou, "A novel genetic service function deployment management platform for edge computing," *Mobile Inf. Syst.*, vol. 2020, pp. 1–22, Oct. 2020.

[6] M. Shahverdy, M. Fathy, R. Berangi, and M. Sabokrou, "Driver behavior detection and classification using deep convolutional neural networks," *Expert Syst. Appl.*, vol. 149, Jul. 2020, Art. no. 113240.

[7] A. Klusek, M. Kurdziel, M. Paciorek, P. Wawryka, and W. Turek, "Driver profiling by using LSTM networks with Kalman filtering," in *Proc. IEEE Intell. Vehicles Symp. (IV)*, Jun. 2018, pp. 1983–1988.

[8] C. Huang, X. Wang, J. Cao, S. Wang, and Y. Zhang, "HCF: A hybrid CNN framework for behavior detection of distracted drivers," *IEEE Access*, vol. 8, pp. 109335–109349, 2020.

[9] A. Engelbert and R. Mirwani, "Vehicle-in-the-loop with sensor fusion testing for efficient ADAS and AD tests," *ATZelectronics Worldwide*, vol. 14, no. 12, pp. 84–89, Dec. 2019.

[10] D. L. Zhang, L. Y. Xiao, Y. Wang, and G. Z. Huang, "Study on vehicle fire safety: Statistic, investigation methods and experimental analysis," *Saf. Sci.*, vol. 117, pp. 194–204, Aug. 2019.

[11] R. Fu, H. Wang, and W. Zhao, "Dynamic driver fatigue detection using hidden Markov model in real driving condition," *Expert Syst. Appl.*, vol. 63, pp. 397–411, Nov. 2016.

[12] S. Al-Sultan, A. H. Al-Bayatti, and H. Zedan, "Context-aware driver behavior detection system in intelligent transportation systems," *IEEE Trans. Veh. Technol.*, vol. 62, no. 9, pp. 4264–4275, May 2013.

[13] C. Miyajima and K. Takeda, "Driver-behavior modeling using on-road driving data: A new application for behavior signal processing," *IEEE Signal Process. Mag.*, vol. 33, no. 6, pp. 14–21, Nov. 2016.

[14] H.-J. Zimmermann, "Fuzzy sets–basic definitions," in *Fuzzy Set Theory—and its Applications*, 4th ed., H.-J. Zimmermann, Ed. Dordrecht, The Netherlands: Springer, 2011, ch. 2, pp. 11–16.

[15] W. De Mulder, S. Bethard, and M.-F. Moens, "A survey on the application of recurrent neural networks to statistical language modeling," *Comput. Speech Lang.*, vol. 30, no. 1, pp. 61–98, 2015.

[16] S. Hochreiter and J. Schmidhuber, "Long short-term memory," *Neural Comput.*, vol. 9, no. 8, pp. 1735–1780, 1997.

[17] J. H. Tan, Y. Hagiwara, W. Pang, I. Lim, S. L. Oh, M. Adam, R. S. Tan, M. Chen, and U. R. Acharya, "Application of stacked convolutional and long short-term memory network for accurate identification of CAD ECG signals," *Comput. Biol. Med.*, vol. 94, pp. 19–26, Mar. 2018.

[18] J. Zhang, J. Yan, D. Infield, Y. Liu, and F.-S. Lien, "Short-term forecasting and uncertainty analysis of wind turbine power based on long short-term memory network and Gaussian mixture model," *Appl. Energy*, vol. 241, pp. 229–244, May 2019.

[19] H. Bousqaoui, S. Achchab, and K. Tikito, "Machine learning applications in supply chains: Long short-term memory for demand forecasting," in *Proc. Int. Conf. Cloud Comput. Technol. Appl.* Cham, Switzerland: Springer, 2017, pp. 301–317.

[20] J. C. Kim and K. Chung, "Prediction model of user physical activity using data characteristics-based long short-term memory recurrent neural networks," *KSII Trans. Internet Inf. Syst.*, vol. 13, no. 4, pp. 2060–2077, Apr. 2019.

[21] A. Krizhevsky, I. Sutskever, and G. E. Hinton, "ImageNet classification with deep convolutional neural networks," in *Proc. Adv. Neural Inf. Process. Syst. (NIPS)*, vol. 25, Dec. 2012, pp. 1097–1105.
[22] M.-C. Popescu, V. E. Balas, L. Perescu-Popescu, and N. Mastorakis, "Multilayer perceptron and neural networks," *WSEAS Trans. Circuits Syst.*, vol. 8, no. 7, pp. 579–588, 2009.
[23] T. N. Sainath, O. Vinyals, A. Senior, and H. Sak, "Convolutional, long short-term memory, fully connected deep neural networks," in *Proc. IEEE Int. Conf. Acoust., Speech Signal Process. (ICASSP)*, Apr. 2015, pp. 4580–4584.
[24] S. Xingjian, Z. Chen, H. Wang, D.-Y. Yeung, W.-K. Wong, and W.-C. Woo, "Convolutional LSTM network: A machine learning approach for precipitation nowcasting," in *Proc. Adv. Neural Inf. Process. Syst.*, 2015, pp. 802–810.
[25] S. Ma and R. Tourani, "Predictive and causal implications of using Shapley value for model interpretation," in *Proc. KDD Workshop Causal Discovery*, 2020, pp. 23–38.
[26] W. Zheng and G. Chen, "An accurate gru-based power time-series prediction approach with selective state updating and stochastic optimization," *IEEE Trans. Cybern.*, early access, Nov. 13, 2021, doi: 10.1109/TCYB.2021.3121312.
[27] Y. Yang, J. Yan, J. Guo, Y. Kuang, M. Yin, S. Wang, and C. Ma, "Driving behavior analysis of city buses based on real-time GNSS traces and road information," *Sensors*, vol. 21, no. 3, p. 687, Jan. 2021.
[28] S. Ucar, B. Hoh, and K. Oguchi, "Abnormal driving behavior detection system," in *Proc. IEEE 93rd Veh. Technol. Conf. (VTC-Spring)*, Apr. 2021, pp. 1–6.
[29] Z. E. A. Elassad, H. Mousannif, H. Al Moatassime, and A. Karkouch, "The application of machine learning techniques for driving behavior analysis: A conceptual framework and a systematic literature review," *Eng. Appl. Artif. Intell.*, vol. 87, Jan. 2020, Art. no. 103312.
[30] S. Arumugam and R. Bhargavi, "A survey on driving behavior analysis in usage based insurance using big data," *J. Big Data*, vol. 6, no. 1, pp. 1–21, Dec. 2019.
[31] W. Rongben, G. Lie, T. Bingliang, and J. Lisheng, "Monitoring mouth movement for driver fatigue or distraction with one camera," in *Proc. 7th Int. IEEE Conf. Intell. Transp. Syst.*, Oct. 2004, pp. 314–319.
[32] B. G. Pratama, I. Ardiyanto, and T. B. Adji, "A review on driver drowsiness based on image, bio-signal, and driver behavior," in *Proc. 3rd Int. Conf. Sci. Technol. Comput. (ICST)*, Jul. 2017, pp. 70–75.
[33] A. Kashevnik, I. Lashkov, and A. Gurtov, "Methodology and mobile application for driver behavior analysis and accident prevention," *IEEE Trans. Intell. Transp. Syst.*, vol. 21, no. 6, pp. 2427–2436, Jun. 2019.
[34] N. Deo, A. Rangesh, and M. M. Trivedi, "How would surround vehicles move? A unified framework for maneuver classification and motion prediction," *IEEE Trans. Intell. Vehicles*, vol. 3, no. 2, pp. 129–140, Jun. 2018.
[35] C.-P. Hwang, M.-S. Chen, C.-M. Shih, H.-Y. Chen, and W. K. Liu, "Apply Scikit-learn in Python to analyze driver behavior based on OBD data," in *Proc. 32nd Int. Conf. Adv. Inf. Netw. Appl. Workshops (WAINA)*, May 2018, pp. 636–639.
[36] N. Kuge, T. Yamamura, O. Shimoyama, and A. Liu, "A driver behavior recognition method based on a driver model framework," *SAE Trans.*, vol. 109, pp. 469–476, Jan. 2000.
[37] Y. Yao, X. Zhao, Y. Wu, Y. Zhang, and J. Rong, "Clustering driver behavior using dynamic time warping and hidden Markov model," *J. Intell. Transp. Syst.*, vol. 25, no. 3, pp. 249–262, May 2021.
[38] G. Castignani, T. Derrmann, R. Frank, and T. Engel, "Driver behavior profiling using smartphones: A low-cost platform for driver monitoring," *IEEE Intell. Transp. Syst. Mag.*, vol. 7, no. 1, pp. 91–102, Sep. 2015.
[39] A. Aksjonov, P. Nedoma, V. Vodovozov, E. Petlenkov, and M. Herrmann, "Detection and evaluation of driver distraction using machine learning and fuzzy logic," *IEEE Trans. Intell. Transp. Syst.*, vol. 20, no. 6, pp. 2048–2059, Aug. 2018.
[40] H. R. Eftekhari and M. Ghatee, "A similarity-based neuro-fuzzy modeling for driving behavior recognition applying fusion of smartphone sensors," *J. Intell. Transp. Syst.*, vol. 23, no. 1, pp. 72–83, Jan. 2019.
[41] S. Arefnezhad, S. Samiee, A. Eichberger, and A. Nahvi, "Driver drowsiness detection based on steering wheel data applying adaptive neuro-fuzzy feature selection," *Sensors*, vol. 19, no. 4, p. 943, Feb. 2019.
[42] C. Ou, C. Ouali, S. M. Bedawi, and F. Karray, "Driver behavior monitoring using tools of deep learning and fuzzy inferencing," in *Proc. IEEE Int. Conf. Fuzzy Syst. (FUZZ-IEEE)*, Jul. 2018, pp. 1–7.
[43] S. Wu, X. Xiao, Q. Ding, P. Zhao, Y. Wei, and J. Huang, "Adversarial sparse transformer for time series forecasting," in *Proc. Adv. Neural Inf. Process. Syst.*, vol. 33, 2020, pp. 17105–17115.

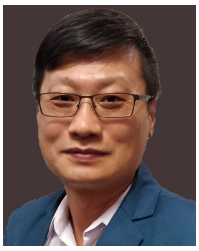

**DAVID CHUNHU LI** (Member, IEEE) received the M.S. degree in information technology application from Monash University, Melbourne, Australia, and the Ph.D. degree in computer science and information engineering from the National Central University, Taoyuan, Taiwan.

He used to serve as the Chief Researcher with the Research and Development Department, the Deputy Manager of Data Science, and the Director of Advanced Technology Office at Foxconn TransIOT Technology Company Ltd. With nearly 20 years of working experience in the information industry, he has published dozens of cited journal and conference papers, and holds six patents. He is currently an Assistant Professor with the International College, Ming Chuan University. His research interests include time series analysis, the Internet of Things, the Internet of Vehicles, big data analysis, artificial intelligence applications, cloud computing, edge computing, software engineering, and software project management. His awards and honors include the Foreign Senior Professionals in the Internet of Things, Internet of Vehicles, and Artificial Intelligence (Ministry of Science and Technology of Taiwan) and the Excellent Paper Award (WASN).

**MICHAEL YU-CHING LIN** received the Master of Information Systems Management degree from Carnegie Mellon University, USA, and the Ph.D. degree in information management from the National Taiwan University, Taiwan. He used to serve as the Director of Applied Computing Program, Ming Chuan University. He is currently an Assistant Professor with the International College, Ming Chuan University, and the university's Director of the Industry-Academia Collaboration and University Extension Division. His research interests include ecommerce, information management, and online user behaviors.

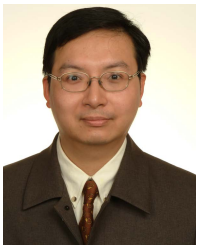

**LI-DER CHOU** (Member, IEEE) received the M.S. and Ph.D. degrees in electronic engineering from the National Taiwan University of Science and Technology, Taiwan, in 1991 and 1995, respectively.

He is currently a Distinguished Professor with the Department of Computer Science and Information Engineering, National Central University, Taiwan, where he is also the Secretary-General. He was the Director of the Computer Center at the National Central University, from 2017 to 2019, and the Director of the Board of Taiwan Network Information Center, from 2014 to 2017. He was also the Deputy Director General of the National Center for High-Performance Computing, Taiwan, from 2013 to 2016. He holds five U.S. and 16 Taiwan invention patents. His research interests include SDN/NFV/SFC, vehicular networks, network management, broadband wireless networks, and internet services. He has published more than 250 articles in these areas. He was a recipient of seven best paper awards and four excellent paper awards from the international and domestic conferences. He was also a recipient of two gold medal awards and four silver medal awards in international invention shows held in Geneva, Moscow, London, and Taipei.